

1  
2  
3  
4  
5  
6  
7  
8  
9  
10  
11  
12  
13  
14  
15  
16  
17  
18  
19  
20  
21  
22  
23  
24  
25  
26  
27  
28  
29  
30  
31  
32  
33  
34  
35  
36  
37  
38  
39  
40  
41  
42  
43  
44  
45  
46  
47  
48  
49  
50  
51  
52  
53  
54  
55  
56  
57  
58  
59  
60

# Slice-selective NMR – a non-invasive method for the analysis of separated pyrolysis fuel samples

*Robert Evans<sup>†\*</sup>, Aran Sandhu<sup>†</sup>, Tony Bridgwater<sup>‡</sup> and Katie Chong<sup>‡</sup>*

<sup>†</sup> Aston Institute of Materials Research, School of Engineering and Applied Science, Aston  
University, Birmingham, B4 7ET, UK, United Kingdom.

<sup>‡</sup> European Bioenergy Research Institute, Aston University, Aston Triangle, Birmingham B4  
7ET, United Kingdom

1  
2  
3 ABSTRACT  
4  
5  
6

7 Pyrolysis oil has been identified as a possible alternative fuel source, however widespread use is  
8 hindered by high acidity and water content. These negative characteristics can be mitigated by  
9 blending with, for example, biodiesel, marine gas oil and butanol. These blended samples can be  
10 unstable and often separate into two distinct phases. NMR spectroscopy is a well-established  
11 spectroscopic technique that is finding increasing application in the analysis of pyrolysis oil and  
12 blended fuels derived from it. Here, slice-selective NMR, where the NMR spectrum of only a  
13 thin slice of the total sample is acquired, is used to study, non-invasively, how the constituent  
14 components of blended biofuel samples are partitioned between the two layers. Understanding  
15 the outcome of the phase separation is an important step towards understanding why the blended  
16 oil samples separate, and may provide answers to mitigating and eventually solving the problem.  
17 The NMR method was successfully used to analyse a number of separated biofuel samples -  
18 typically separated into an oil layer, containing marine gas oil and biodiesel, above a bio-oil  
19 layer with a high water and butanol content.  
20  
21  
22  
23  
24  
25  
26  
27  
28  
29  
30  
31  
32  
33  
34  
35  
36  
37  
38  
39  
40  
41  
42  
43  
44  
45  
46  
47  
48  
49  
50  
51  
52  
53  
54  
55  
56  
57  
58  
59  
60

## INTRODUCTION

With concerns over limited supplies of fossil fuels and their effect on atmospheric carbon dioxide, research into alternative fuel sources has become increasingly important and timely. The use of biomass has been introduced as a solution toward the development of sustainable and green energy platforms.<sup>1,2</sup> Biomass pyrolysis is a thermochemical conversion process, involving irreversible heat-driven decomposition of lignocellulosic biomass in the absence of oxygen.<sup>3</sup> The starting material, lignocellulose, is a complex mixture comprising of several key polymeric constituents (in particular, lignin, cellulose, hemicellulose) and pyrolysis depolymerises these into smaller molecules. The pyrolysis products contain char, gas, and a pyrolysis oil, a complex mixture of alcohols, aldehydes, alkenes, carbohydrates, carboxylic acids, esters, furans, guaiacols, ketones, nitrogen compounds, miscellaneous oxygenates, phenols, syringols and water.<sup>3-5</sup> Pyrolysis oil (bio-oil) can be used as a fuel for boilers but it cannot be used directly as a transportation fuel in unmodified engines. It is typically too acidic and contains too much water. There are a number of methods by which the utility of a pyrolysis product can be improved,<sup>6-8</sup> such as by blending with other products.<sup>9-13</sup> In the system studied here, the bio-oil is blended with butan-1-ol, marine gas oil and rapeseed methyl ester (biodiesel or fatty acid methyl ester (FAME)) to make a final fuel product. Being both sustainable and renewable, fuels incorporating blended biofuels offer features which allow them to work within existing infrastructure and thus represent a short-term alternative to fossil fuels.

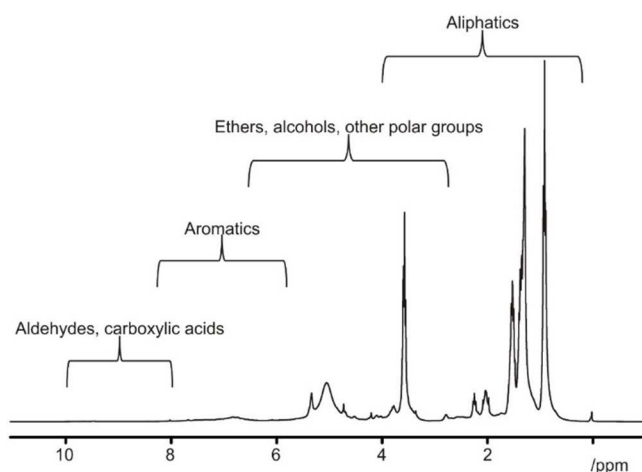
These multiple component blends are typically opaque and can readily separate into a multiple-phase solution.<sup>12-14</sup> A key challenge to the successful blending of these fuel products is the

1  
2  
3 understanding and mitigation of this phase separation. Once separated, the blends are not suitable  
4 as fuel products and could cause significant damage to an engine if used. While the separation of  
5 these blends has been reported, to the best of our knowledge there is no work investigating, in  
6 detail, why phase separation occurs, or if there is any migration of the compounds between the  
7 phase separated layers. Understanding how the different components of the blended fuel interact  
8 with the solvents and co-solutes, and which components remain in which layers, will provide a  
9 step forward in the understanding of bio-oil miscibility. This will, in turn, lead to the production  
10 of stable fuel blends and may provide answers to mitigating and eventually solving this problem.  
11  
12  
13  
14  
15  
16  
17  
18  
19  
20  
21  
22

23 A number of techniques are currently used to analyse bio-oil based samples.<sup>15,16</sup> Chemical  
24 analysis of the samples provides quantitative information about the water content and pH, key  
25 parameters for the utility of the final oil blend. The acid number of the sample, the mass of  
26 potassium hydroxide (KOH) in milligrams that is required to neutralize one gram of chemical  
27 substance, is related to the sample pH. The viscosity can be measured using a viscometer. Other  
28 analytical techniques include chromatography - gas chromatography (GC)<sup>17</sup>, high-performance  
29 liquid chromatography (HPLC)<sup>18</sup> and gel permeation chromatography (GPC)<sup>19</sup> - and  
30 spectroscopy.<sup>20</sup> Chromatographic methods are inherently invasive and destructive. Of the  
31 spectroscopic methods available, FT-IR allows for the quantitative measurement of functional  
32 groups and nuclear magnetic resonance (NMR) gives a quantitative, chemically selective,  
33 measurement of all chemical species present in a sample.  
34  
35  
36  
37  
38  
39  
40  
41  
42  
43  
44  
45  
46  
47  
48  
49

50 NMR is a non-invasive technique that is near ubiquitous in chemical science. The intensities of  
51 the signals recorded are proportional to the number of spins in that environment, making it  
52 quantitative. <sup>1</sup>H nuclei are highly abundant, overcoming the inherently low sensitivity of the  
53 technique. The resonant frequencies observed allow for the species present in the sample to be  
54  
55  
56  
57  
58  
59  
60

1  
2  
3 identified on the basis of their chemistry and the functional groups present (Fig. 1). More polar  
4 or unsaturated groups present typically lead to signals at higher chemical shift. The application  
5 of NMR to pyrolysis oils is a well-established technique<sup>20</sup> and has very recently been reviewed.<sup>21</sup>  
6  
7  
8  
9  
10



30  
31 **Figure 1.** <sup>1</sup>H NMR spectra of a blended fuel sample, with characteristic chemical shift regions of  
32 functional groups indicated.  
33  
34  
35

36 The analysis of these samples is highly complicated by severe overlapping of the spectral  
37 features. All species present contribute to the signals observed, making deconvolution and  
38 interpretation dependent on 2-dimensional techniques or software packages<sup>22</sup>. The NMR analysis  
39 of separated samples would be difficult to achieve without physical separation of the two phases.  
40 Standard 1D NMR measurements of the separated sample will sum the signals of the two phases  
41 together and the spectral resolution and quality would be detrimentally affected by the presence  
42 of the boundary.  
43  
44  
45  
46  
47  
48  
49  
50  
51  
52  
53  
54  
55  
56  
57  
58  
59  
60

1  
2  
3 NMR spectrometers are now fitted with pulsed magnetic field gradients as standard. While these  
4  
5 are typically used to rapidly acquire good quality multi-dimensional NMR spectra<sup>23</sup>, they also  
6  
7  
8 allow the acquisition of NMR data with spatial information, such as diffusion NMR<sup>24,25</sup> and  
9  
10 spatially-resolved or slice-selective NMR<sup>26</sup>. Diffusion NMR allows for the components of a  
11  
12 mixture to be resolved according to their diffusion coefficient, producing a pseudo-  
13  
14 chromatographic separation of the sample. The use of diffusion NMR has already been suggested  
15  
16 as a potential tool for bio-oil analysis.<sup>21</sup>  
17  
18  
19  
20  
21  
22  
23

24 Slice-selective NMR is a technique similar to those widely used in magnetic resonance imaging  
25  
26 but has not found wide use outside of this context. Its use in 1-dimensional chemical applications  
27  
28 has been demonstrated in a number of inhomogeneous systems, including idealised systems such  
29  
30 as benzene floating on water<sup>26</sup> or water and olive oil systems<sup>27</sup> and the diffusion of small  
31  
32 molecules in non-equilibrium systems, including CO<sub>2</sub> in ionic liquid<sup>28</sup> and small molecules such  
33  
34 as caffeine in gels.<sup>29,30</sup> Its use is not limited to observing <sup>1</sup>H, with application to the study of <sup>7</sup>Li  
35  
36 ions in both polymer gels<sup>31,32</sup> and in systems intended to resemble Li-ion batteries.<sup>33</sup> Excitation  
37  
38 of a given slice of the sample is accomplished by applying a long, soft radiofrequency pulse in  
39  
40 the presence of a pulsed magnetic field gradient. During the field gradient ( $G$ ; on most standard  
41  
42 NMR probes, this is applied along the direction of the magnetic field or  $z$ -axis), all resonance  
43  
44 frequencies experience an offset,  $\Omega$ , that depends on the vertical deviation ( $z$ ) from the centre of  
45  
46 the gradient coil, see Equation (1).  
47  
48  
49  
50  
51  
52  
53  
54  
55  
56  
57  
58  
59  
60

$$\Omega = \frac{\gamma G_z z}{2\pi}$$

Equation (1)

1  
2  
3 A soft pulse, with a bandwidth  $\Delta B$ , employed at this offset will selectively excite a horizontal  
4 slice of the sample, centred at  $z$ , with a thickness  $\Delta z$  obtained from Equation (2).  
5  
6  
7

$$\Delta z = \frac{2\pi}{\gamma G_z} \Delta B$$

8  
9  
10  
11  
12  
13  
14  
15 Equation (2)  
16  
17

18 Only this thin horizontal slice of the sample is excited by the soft radiofrequency pulse (Fig. 2).  
19  
20 Before acquisition of the NMR data, the field gradient is switched off and all spins are detected  
21 with their normal resonance frequencies. The pulse bandwidth is much larger than typical  
22 spectral widths and  $^1\text{H}$  NMR spectra can be obtained for that particular slice of the sample but  
23 with a reduced signal-to-noise ratio. The pulse sequence code used and a schematic of the  
24 sequence can be found in the SI.  
25  
26  
27  
28  
29  
30  
31

32  
33 This work demonstrates the use of slice-selective NMR techniques in analysing phase-separated  
34 bio-fuel mixtures. The technique can be applied on any commercial NMR spectrometer, as long  
35 as it is equipped with pulsed field gradients. This report represents what is, to the best of our  
36 knowledge, the first use of slice-selective NMR methodology applied to biofuel mixtures and is  
37 used to give chemical information about the components present in the two phases of the phase  
38 separated blended samples studied here.  
39  
40  
41  
42  
43  
44  
45  
46  
47  
48  
49  
50  
51  
52  
53  
54  
55  
56  
57  
58  
59  
60

## EXPERIMENTAL

### Materials and Samples

Eight blended biofuel samples containing differing amounts of the bio-oil, marine gas oil, fatty acid methyl ester and butanol were analysed. All blended samples contained both bio-oil and butanol and either or both of the other components, and are referred to as three- or four-component mixtures. Figure 2 shows two typical blended fuel samples. A photograph of all eight samples, and a table of their compositions, is provided in the ESI.



**Figure 2.** Photograph of two typical blended fuel samples.

The blends were prepared by adding a weighed sample of bio-oil to butanol in a sample container, followed by biodiesel and/or MGO. Finally the solvent was added, the container sealed and lightly shaken. All blends were prepared at room temperature with a total weight of 20 grams. The samples were left to settle for 48hrs before visual inspection to establish



1  
2  
3 homogeneity. The blends in this study have all been studied previously and tested for key  
4  
5 characteristics that give an indication of their suitability for engine testing.<sup>12</sup>  
6  
7

## 8 9 **NMR Experiments**

10  
11  
12 All <sup>1</sup>H NMR measurements were performed on a 300 MHz Bruker Avance spectrometer at 298  
13  
14 K, using a 5 mm BBO probe equipped with a z gradient coil producing a maximum gradient  
15  
16 strength of 0.55 T m<sup>-1</sup>. For the slice-selective NMR experiments, a G4 cascade<sup>34</sup> was used for  
17  
18 the selective pulse, with a 5000 Hz bandwidth and applied at offsets of + and - 5000 Hz,  
19  
20 corresponding to the upper and lower layers respectively. A gradient of 5 % of the maximum  
21  
22 gradient strength was applied concurrently with the selective pulse. This corresponds to a slice  
23  
24 4.3 mm in width, exciting a slice centred 4.3 mm from the centre of the *G<sub>z</sub>* coils. 1D <sup>1</sup>H  
25  
26 experiments of blended, separated and the decanted layers of the separated samples were also  
27  
28 acquired. No deuterated solvents were added to the samples. All NMR experiments were  
29  
30 acquired without the use of the lock and shimming was achieved using the area of the acquired  
31  
32 FID. The data presented here were all acquired with 64 scans, for an experimental duration of 4  
33  
34 minutes for the slice-selective pulse sequence and 2 minutes 30 seconds for a standard proton  
35  
36 experiment, and all data were processed using TopSpin.  
37  
38  
39  
40  
41  
42  
43

44 The NMR analysis of the oils was done blind. The identities and compositions of the oils were  
45  
46 only revealed to the NMR spectroscopists after the analysis of the NMR spectra was completed.  
47  
48  
49  
50  
51  
52  
53  
54  
55  
56  
57  
58  
59  
60

## RESULTS AND DISCUSSION

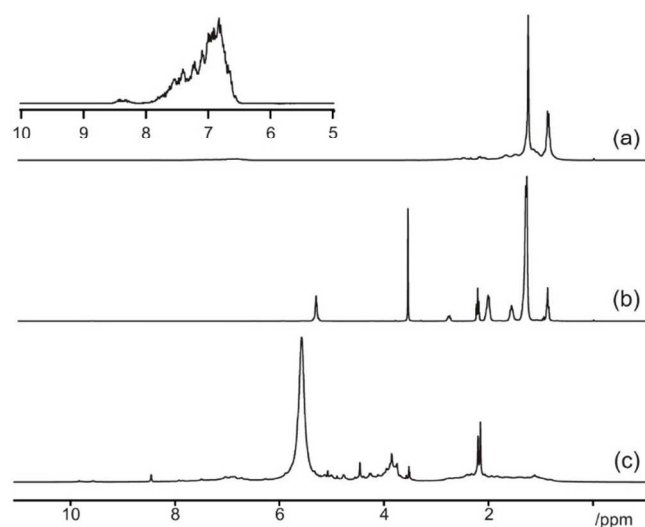
### <sup>1</sup>H NMR of Raw Materials

1D <sup>1</sup>H spectra were acquired for marine gas oil, fatty acid methyl ester and bio-oil prior to blending with butanol. These samples are all themselves complex mixtures containing a wide range of species, with different functionalities, over several orders of concentrations. However, some qualitative analysis of the chemical species can be made from these spectra. Figure 3 depicts spectra for the three components, with an enlargement of the aromatic region of marine gas oil.

**Marine gas oil:** Marine gas oil is made from the distillate fraction of petroleum oil. It is the fuel most commonly used for inland marine transport. It has been demonstrated that biodiesel and marine gas oil are miscible in all proportions. The unsaturated alkyl chains give large signals at 0.9 ppm and 1.4 ppm. There are a number of minor components present within the component, with the signals observed between 6.5 ppm and 8 ppm indicating the presence of aromatic species. The MGO used in this study was supplied by Statoil in Norway

**Fatty Acid Methyl Ester (biodiesel, FAME):** A key component of the blended fuel is the methyl ester of a long chain fatty acid. The biodiesel used for this study was produced through the transesterification of pure rape seed oil in order to yield rape methyl esters. The signals at low chemical shift are consistent with a long alkyl chain terminated by esterification with methanol. The methyl group of ester produces a singlet peak at ~ 5.3 ppm. There is a very low-intensity singlet at 10 ppm indicating the presence of some unreacted carboxylic acid.

1  
2  
3  
4  
5  
6  
7 **Bio-oil:** A component of all of the blends is fast pyrolysis oil (bio-oil). The bio-oil used in this  
8  
9 work is a mixture of phenolic compounds, carboxylic acids and water. There is a characteristic  
10 pair of peaks at  $\sim 2.1$  ppm. The high acidity of the sample shifts the large water peak to 5.5 ppm.  
11  
12 The peaks found between 9 and 10 ppm are likely to arise from the presence of carboxylic acids.  
13  
14 The peaks found between 9 and 10 ppm are likely to arise from the presence of carboxylic acids.  
15  
16 The bio-oil used in the samples was produced at Aston University using a Norwegian Spruce  
17  
18 feedstock in a  $1 \text{ kg h}^{-1}$  fast pyrolysis rig.  
19  
20  
21



41 **Figure 3.** 1D  $^1\text{H}$  NMR spectra of raw components (a) marine gas oil (b) FAME and (c) bio-oil  
42 used in blended bio-fuel mixtures. Inset in Fig. 3 (a) shows a hundred fold expansion of the  
43 region between 5 and 10 ppm, indicating the signals due to aromatic species in the marine gas  
44  
45  
46  
47  
48  
49  
50  
51  
52  
53  
54  
55  
56  
57  
58  
59  
60

## $^1\text{H}$ NMR of Unseparated Samples

Standard 1D  $^1\text{H}$  spectra were also acquired for a number of blended samples, containing both three (Fig. 4) and four (Fig. 5) of the possible components. All samples, A – E, contained bio-oil and butanol.

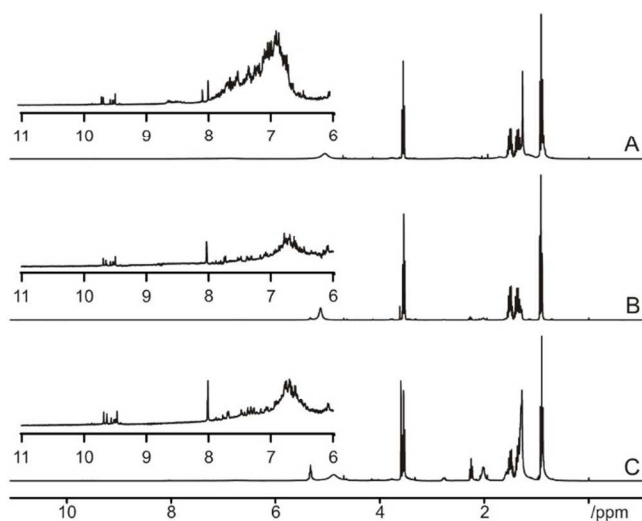


**Figure 4.** 1D  $^1\text{H}$  NMR spectra of three-component unseparated samples, A, B and C.

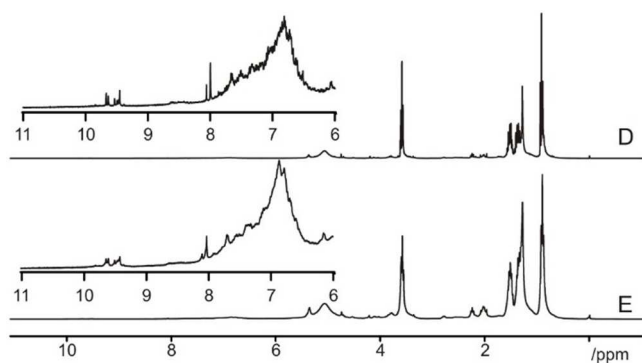


**Figure 5.** 1D  $^1\text{H}$  NMR spectra of four-component unseparated samples, D and E.

1  
2  
3  
4  
5  
6  
7 Quantitative analysis of the mixtures is hindered by the overlap of signals from the various  
8  
9 components of the mixtures used in this study. It is, however, possible to identify the  
10  
11 components present in the samples. While the chemical shifts of peaks do depend on the local  
12  
13 environment and will change as a function of solvent composition and pH, each component has a  
14  
15 number of distinctive peaks, with multiplet structure, which can be identified in the acquired  
16  
17 spectra. Qualitative analysis and assignment of the peaks can be used to identify which  
18  
19 components are present in the samples, as summarised in Table 1. The three, three-component  
20  
21 unseparated samples (A – C) all contain bio-oil and butanol, plus either FAME or marine gas oil.  
22  
23 The multiplets due to the protons on the  $\beta$  and  $\gamma$  carbons of butanol can be clearly observed at ~  
24  
25 1.5 ppm for all three samples. The water contained within the bio-oil produces a broad water  
26  
27 peak at ~ 5 ppm, higher than typically observed for water in water but lower than the observed  
28  
29 water peak in the raw bio-oil. Another distinctive set of signals produced by the bio-oil are  
30  
31 found between 9 and 10 ppm, with this set of signals observed in all of samples A-E.  
32  
33  
34  
35  
36  
37

38  
39 In samples B and C, the presence of multiplets at ~2.0 ppm and ~5.3 ppm and a triplet at ~2.3  
40  
41 ppm confirm the presence of FAME, while the absence of marine gas oil is confirmed by the  
42  
43 absence of the aromatic signals and the large, sharp peak, due to  $-\text{CH}_2-$  groups, observed at ~1.2  
44  
45 ppm. Samples D and E contain all four constituent liquids and distinctive peaks belonging to  
46  
47 each are observed in both spectra. This analysis of the unseparated samples was used as a basis  
48  
49 for the later analysis of the separated samples.  
50  
51  
52  
53  
54  
55  
56  
57  
58  
59  
60

Sample	Butanol	Bio-Oil	Water	Marine gas oil	FAME
A	×	×	×	×	
B	×	×	×		×
C	×	×	×		×
D	×	×	×	×	×
E	×	×	×	×	×

**Table 1.** Summary of components present in samples A, B, C, D and E as determined by 1D  $^1\text{H}$  NMR analysis.

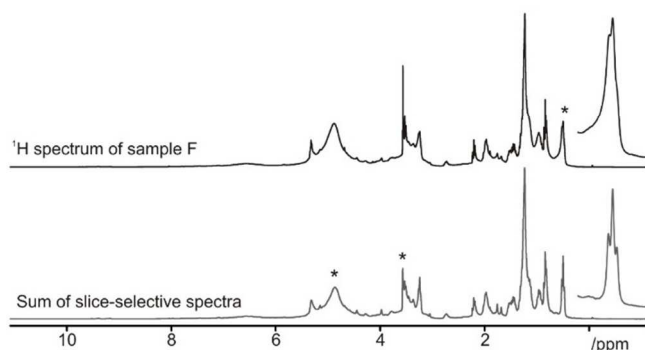
### Accuracy of Slice-Selective Pulse Sequence

The NMR spectra produced by the slice-selective pulse sequence are of no use if they do not achieve two key requirements (a) that they correspond to the spectra of physically separated samples and (b) that the two slices reproduce that of the full sample. While (b) might not be completely achieved due to relaxation of signals with short  $T_2$  times and any inhomogeneities in the sample, it should still be possible to compare a sum of the spectra of the two slices with that of the whole sample.

For sample F, one of the separated samples studied here, the sum of the upper and lower levels was compared with the spectrum for the whole sample to demonstrate that the near completeness of the method (Fig. 6). The key features of the spectrum of the whole sample are reproduced, but

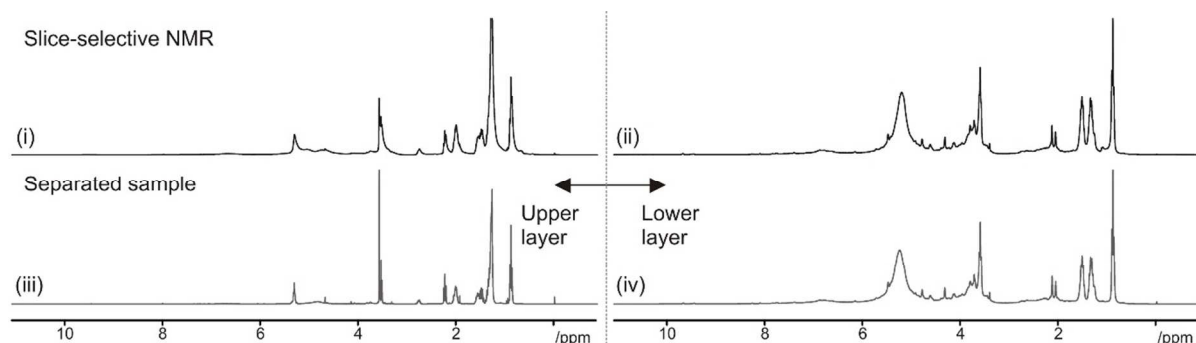
1  
2  
3 there are some key differences. An advantage of the slice-selective approach is that more highly  
4 resolved spectra can be obtained for the slices than for the whole sample. Inhomogeneities in  
5  
6 resolved spectra can be obtained for the slices than for the whole sample. Inhomogeneities in  
7  
8 samples, such as the boundary between the two layers, lead to poorly shimmed spectra of the  
9  
10 samples. By acquiring data from only a small slice of the sample, away from the boundary,  
11  
12 higher resolution spectra can be acquired for the separated regions of the sample. The triplet peak  
13 of butanol at 0.55 ppm, indicated by an asterisk in the top spectrum of Figure 6, is resolved using  
14  
15 the slice selective technique, while it is not resolved in spectra acquired using a standard proton  
16  
17 experiment.  
18  
19  
20  
21  
22

23  
24 Certain peaks, notably the broad water peak, exhibit reductions in their intensities in the sum  
25  
26 of the slices compared to the spectrum of the whole sample. This is likely due to these signals,  
27  
28 denoted by asterisks in the spectra of the sum, having short  $T_2$  times and experiencing some  
29  
30 relaxation during the duration of the experiment. The duration of the G4 cascade used throughout  
31  
32 is 1566.8  $\mu\text{s}$ , long enough for spins with very short  $T_2$  times to exhibit some losses.  
33  
34  
35  
36



50 **Figure 6.** Comparison of the sum of slice-selective  $^1\text{H}$  NMR spectra of upper and lower levels of  
51  
52 Sample F with  $^1\text{H}$  NMR spectrum of complete sample. Butanol peak at 0.55 ppm enlarged to  
53  
54 highlight differences in resolution between the two techniques.  
55  
56  
57  
58  
59  
60

1  
2  
3  
4 A comparison of the slice-selective NMR approach with spectra obtained from the carefully  
5  
6 decanted upper and lower layers of sample F is shown in Figure 7. There is a noticeable  
7  
8 difference between the spectra obtained by the two different approaches. Physically separating  
9  
10 the samples allows for highly resolved, very well shimmed NMR spectra to be obtained.  
11  
12 However, in spite of the poorer resolution, all of the peaks in Fig. 7(iii) can be observed in Fig.  
13  
14 7(i). There are very little differences in resolution of the lower layer and all peaks in Fig. 7(iv)  
15  
16 7(i). There are very little differences in resolution of the lower layer and all peaks in Fig. 7(iv)  
17  
18 are observed in the slice-selective spectrum (Fig. 7(ii)).  
19  
20  
21  
22  
23  
24



25  
26  
27  
28  
29  
30  
31  
32  
33  
34  
35  
36  
37 **Figure 7.** Comparison of slice-selective  $^1\text{H}$  NMR spectra of (i) upper and (ii) lower levels of  
38  
39 Sample F with  $^1\text{H}$  NMR spectra of the (iii) upper and (iv) lower levels of a physically separated  
40  
41 sample.  
42  
43  
44  
45  
46  
47  
48  
49  
50  
51  
52  
53  
54  
55  
56  
57  
58  
59  
60



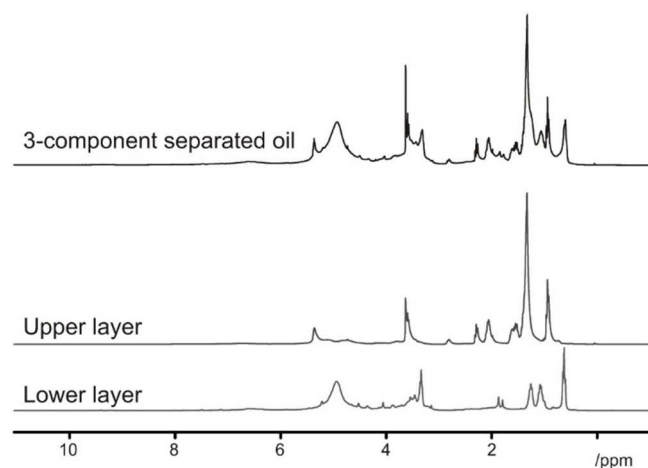
1  
2  
3 Figures 6 and 7 show that the slice-selective pulse sequence is working as intended and that, for  
4  
5 the samples used here, there are neither false positive nor false negative peaks. All key features  
6  
7 of the original spectra are reproduced and the slices accurately represent the composition of the  
8  
9 two different phases.  
10  
11

### 12 13 14 15 16 17 **Slice-Selective NMR of Separated Samples** 18

19  
20 Three of the samples used had separated into two phases (see Fig. 2 and Fig. SI.2). The NMR  
21  
22 spectra of these separated samples were also acquired using both standard 1D  $^1\text{H}$  and slice-  
23  
24 selective  $^1\text{H}$  NMR pulse sequences.  
25  
26

27  
28 Slice-selective  $^1\text{H}$  NMR spectra of the upper and lower phases of the near completely opaque  
29  
30 three-component blended sample F (see Fig. SI.2 for an image of all samples used in this study)  
31  
32 illustrate how the mixture has partitioned between the two layers (Fig. 8). The overlap of the  
33  
34 alkyl peaks of the methyl ester with those of the marine gas oil makes the aliphatic region  
35  
36 difficult to use in these studies but an absence of aromatic peaks (see Figs. 1 and 3) indicates an  
37  
38 absence of the marine gas oil's aromatic species in the layer. The singlet peak, assigned to the  
39  
40 methyl group of the ester, at  $\sim 3.5$  ppm combined with multiplets at  $\sim 2$  and  $\sim 5.3$  ppm indicates  
41  
42 the presence of FAME in the upper layer of the sample. These peaks are not observed in the  
43  
44 lower layer. The butanol can be observed in both layers, albeit with differences in chemical shift,  
45  
46 with the triplet at  $\sim 3.5$  ppm observed in the top layer, partially overlapping with the FAME  
47  
48 singlet. The other three peaks of the butanol are overlap significantly with the FAME signals.  
49  
50 The doublet at 1.8 ppm is assigned to the bio-oil, in spite of now being found at a lower chemical  
51  
52 shift. The water peak found in bio-oil at 5.5 ppm is larger than any observed in the unseparated  
53  
54  
55  
56  
57  
58  
59  
60

1  
2  
3 samples and has moved to a lower chemical shift, albeit one still higher than observed for  
4  
5 ‘normal’ water samples (liquid water typically has a chemical shift of 4.7 ppm<sup>35</sup>). No water peak  
6  
7 is observed in the upper layer. As a result of their typical relative densities, oils are typically  
8  
9 observed in the upper layer. As a result of their typical relative densities, oils are typically  
10  
11 observed to float on water<sup>36</sup>. The separation of the sample into an oil-based top layer containing  
12  
13 FAME and a small amount of butanol over an aqueous/alcohol layer is not unexpected.  
14  
15  
16  
17  
18  
19  
20  
21  
22  
23  
24  
25  
26  
27  
28  
29  
30  
31  
32  
33  
34



35 **Figure 8.** Slice-selective <sup>1</sup>H NMR spectra of Sample F, a phase-separated 3-component oil  
36  
37 sample.  
38  
39

40  
41 Slice-selective <sup>1</sup>H NMR spectra of the upper and lower phases of the four-component separated  
42  
43 sample, G, (Fig. 9) illustrate how the mixture has partitioned between the two layers and the  
44  
45 almost complementary nature of the separation in this case. The two signature peaks of the alkyl  
46  
47 chains present in the marine gas oil can be observed in the upper layer but not in the lower. The  
48  
49 singlet peak at ~ 3.5 ppm is assigned to the methyl group of the ester, while peaks consistent  
50  
51 with those of the fatty acid chain not overlapping with the alkyl peaks can be observed at ~ 2 and  
52  
53 ~ 5.3 ppm. These peaks are not observed in the lower level. The doublet at 1.8 ppm is assigned  
54  
55 to the bio-oil, in spite of now being found at a lower chemical shift. The large water peak found  
56  
57  
58  
59  
60

1  
2  
3 in bio-oil at 5.5 ppm has again moved to a lower chemical shift, albeit one still higher than  
4  
5 observed for 'normal' water samples. Neither water peak nor butanol are observed in the upper  
6  
7 layer. As with the three-component sample analysed previously, the four component sample  
8  
9 separating into an oil-based top layer over an aqueous/alcohol layer is not unexpected.  
10  
11  
12  
13

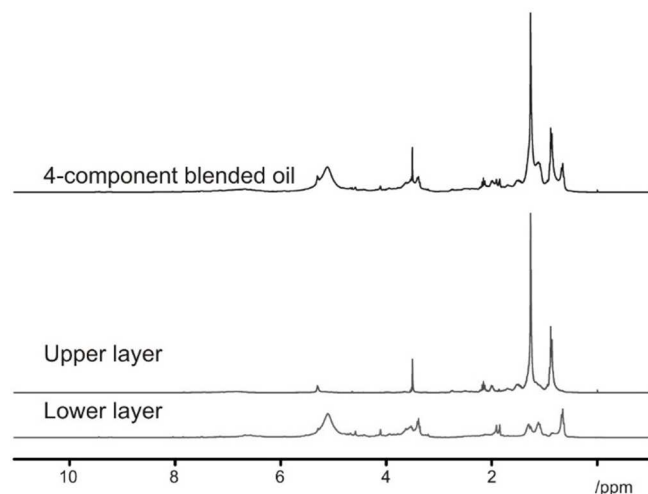


**Figure 9.** slice-selective  $^1\text{H}$  NMR of Sample G, a phase-separated 4-component oil sample.

The aromatic species in the sample, observed at chemical shifts greater than 6 ppm, also separate across the two phases, as shown in Figure 10. Both marine gas oil and bio-oil contain components with peaks in this region, such as aromatic species and carboxylic acids. The 4-component mixture contains both, but there is a near complementary nature to the two layers – components are found in either the upper or the lower layers, not both.

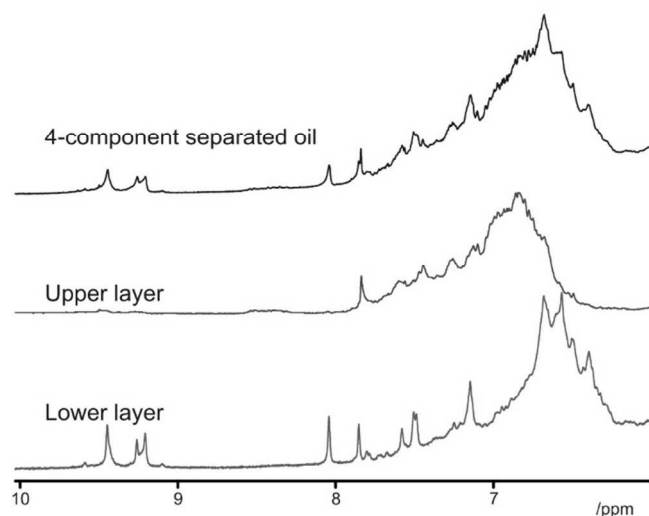


**Figure 10.** Slice-selective  $^1\text{H}$  NMR of aromatic region of Sample G, a phase-separated 4-component oil sample.

Finally, sample H is a three-component sample that has separated. Analysis of the spectra in Figure 11 indicates that butanol is now found in both the upper and lower layers, with the triplet peaks due to the terminal and hydroxyl protons of butan-1-ol, indicated with asterisks in Fig. 11, both observed in the upper layer. None of the FAME peaks, such as the distinctive singlet at 3.5 ppm, are observed, confirming that the sample contains bio-oil, marine gas oil and butanol only.

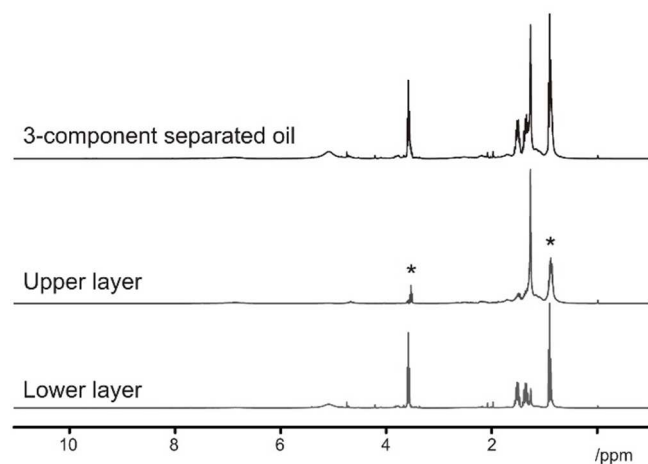


**Figure 11.** Slice-selective <sup>1</sup>H NMR of Sample H, a phase-separated 3-component oil sample.

Table 2 summarises the compositions of the three separated samples, indicating whether a component was identified as present in either the upper or lower layer. The NMR method introduced here gives a quick qualitative description of the composition of the two species. In the cases of sample G, the mixture separates into simple oil/water mixtures. Samples F and H are slightly more complicated, with butanol dissolving into the upper layer.

Sample	Butanol	Bio-Oil	Water	Marine gas oil	Methyl ester
F upper	×				×
F lower	×	×	×		
G upper				×	×
G lower	×	×	×		
H upper	×			×	
H lower	×	×	×		

**Table 2.** Summary of components present in samples F, G and H as determined by 1D  $^1\text{H}$  NMR analysis.

## CONCLUSIONS

This paper presents the use of slice-selective NMR techniques applied to blended bio-oil samples. These samples can be unstable, separating into two distinct phases, and understanding how the sample has separated will give additional insights into preparing stable samples that can be used as future fuel resources.

Most NMR spectrometers are now equipped with the high quality, pulsed field gradients that the method described here requires as standard. The technique described here is non-invasive, and chemically specific allowing for the identification of presence or absence of the various components of the blends. While there are some losses of signal due to transverse relaxation of signals with short  $T_2$  times, the technique could be used in conjunction with more standard quantitative NMR methods, gaining information about, for example, water content from the area of the broad water peak while also identifying the final location of the species concerned. In this particular study, the NMR parameters determining the position and thickness of the slice have been set somewhat conservatively, with a thick slice excited, far away from any boundary between phases. Thinner slices can be acquired, at the expense of signal to noise, and they can be easily moved by changing the offset of the selective pulse. The method is not limited to superconducting magnets; as long as the spectrometer has pulsed field gradients in an appropriate geometry, the method described here should be transferable.

More generally, NMR techniques are not limited to one-dimensional spectra of  $^1\text{H}$  and  $^{13}\text{C}$ .

There is plenty of scope for expansion and development of the technique. A recent review of the field showed how other nuclei can be used to study pyrolysis oils and related fuel sources, as well as 2-dimensional heteronuclear correlation experiments.<sup>21</sup> The slice selective technique

1  
2  
3 could be combined with a wide range of other NMR sequences to acquire chemical data on  
4 inhomogeneous systems. Possible experiments are not limited to just protons. Carbonyl and  
5 hydroxyl groups are key indicators of the suitability of oils for processing, upgrading and later  
6 use. The former can be measured by derivatization of the bio-oil with 4-(trifluoromethyl)-  
7 phenylhydrazine, followed by  $^{19}\text{F}$  NMR spectroscopy.<sup>37</sup> The latter can be studied using  $^{31}\text{P}$  NMR  
8 spectroscopy, following phosphitylation of the sample.<sup>38</sup> Both nuclei could be studied using the  
9 technique presented here, with some modification of the experimental parameters.

10  
11  
12 NMR techniques can also be used to study physical parameters of systems. The  $T_2$  time of a  
13 water peak has been shown to be related to the pH of some micellar systems<sup>39</sup> and could be used  
14 in such a manner in bio-oil-based fuel samples. Diffusion NMR produces information on the  
15 sizes of species present<sup>40</sup> and the viscosity of the sample<sup>41</sup>. Both techniques can be used to filter  
16 out unwanted signals, belonging to either large<sup>42</sup> or small<sup>43</sup> species. These techniques could be  
17 combined with the work presented here to give localised measurements of both unseparated and  
18 separated blended bio-oil samples.

19  
20  
21 Most NMR experiments are typically performed in homogeneous systems, so as to get the  
22 highest resolution in the final spectra. When faced with non-homogeneous samples such as  
23 studied in this work, slice-selective NMR offers a non-invasive method of acquiring chemical  
24 information from the samples. The application studied here is one where slice-selective NMR  
25 techniques could find wide use, as it gives a quick (the experimental duration for acquiring one  
26 slice with 64 scans is less than 4 minutes), spatially selective, chemically informative, non-  
27 invasive indication of what components are found in which layers of the compound. However,  
28 the approach is certainly not limited to just the biphasic samples described here, and will be  
29 applicable to any inhomogeneous sample.



1  
2  
3 In the this work, slice-selective NMR has been used to characterise opaque, phase separated  
4 samples, as well as give chemically specific information about the final compositions of a set of  
5  
6 blended biofuel samples. In the small sample of oils studied here, key differences in the  
7  
8 partitioning between the two layers was observed. With an increasing interest in both biofuel as a  
9  
10 long term, sustainable resource and the use of NMR techniques in studying biofuel samples, the  
11  
12 methodology presented here should find wide use.  
13  
14  
15  
16  
17  
18  
19  
20  
21  
22  
23  
24  
25  
26  
27  
28  
29  
30  
31  
32  
33  
34  
35  
36  
37  
38  
39  
40  
41  
42  
43  
44  
45  
46  
47  
48  
49  
50  
51  
52  
53  
54  
55  
56  
57  
58  
59  
60

1  
2  
3 ASSOCIATED CONTENT  
4  
5

6  
7 **Supporting Information.**  
8

9  
10 Supporting information includes the pulse sequence used in this study and photographs of all  
11  
12 samples studied in this work.  
13  
14

15  
16 AUTHOR INFORMATION  
17

18  
19 **Corresponding Author**  
20

21 Robert Evans, r.evans2@aston.ac.uk  
22  
23

24  
25 **Author Contributions**  
26

27 The manuscript was written through contributions of all authors. All authors have given approval  
28  
29 to the final version of the manuscript.  
30  
31

32  
33 **Funding Sources**  
34

35 Robert Evans and Aran Sandhu received funding from the Royal Society of Chemistry  
36  
37 Analytical Trust Fund.  
38  
39  
40  
41  
42  
43  
44  
45  
46  
47  
48  
49  
50  
51  
52  
53  
54  
55  
56  
57  
58  
59  
60

## ACKNOWLEDGMENT

Rob Evans would like to thank Sarah Lee (now at Birkbeck, University of London) and Peter Gierth (Bruker UK Ltd) for support in developing the NMR techniques used. Aran Sandhu was funded by the Royal Society of Chemistry Analytical Trust Fund Summer Studentship scheme (ACSS 16/023).

## REFERENCES

1. Kamm, B.; Gruber, P.R.; Kamm, M., Eds. *Biorefineries—Industrial Processes and Products: Status Quo and Future Directions. Vol. 1*; Wiley-VCG, 2006.
2. Kamm, B., Gruber, P.R., Kamm, M., Eds. *Biorefineries—Industrial Processes and Products: Status Quo and Future Directions. Vol. 2*; Wiley-VCG, 2006.
3. Bridgwater, A.V. Review of fast pyrolysis of biomass and product upgrading. *Biomass Bioenerg.* **2012**, *38*, 68-94.
4. Bridgwater, A.V. *Fast Pyrolysis of Biomass: A Handbook. Vol. 2*; CPL Press, 2002.
5. Mohan, D; Pittman, Jr., C. U.; Steele P. H. Pyrolysis of Wood/Biomass for Bio-oil: A Critical Review. *Energy Fuels* **2006**, *20* (3), 848-889.
6. Butler, E.; Devlin, G.; Meier, D.; McDonnell, K. A. A review of recent laboratory research and commercial developments in fast pyrolysis and upgrading. *Renew. Sustainable Energy Rev.* **2011**, *15* (8), 4171-4186.

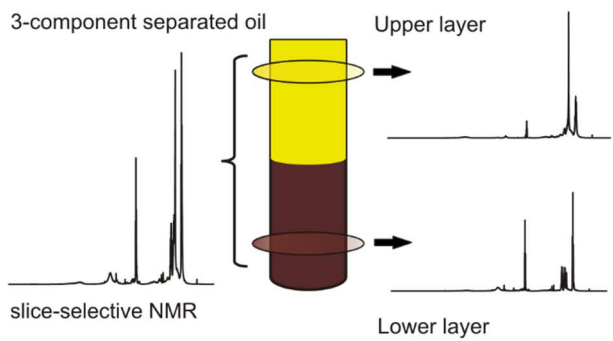
- 1  
2  
3  
4  
5  
6  
7  
8  
9  
10  
11  
12  
13  
14  
15  
16  
17  
18  
19  
20  
21  
22  
23  
24  
25  
26  
27  
28  
29  
30  
31  
32  
33  
34  
35  
36  
37  
38  
39  
40  
41  
42  
43  
44  
45  
46  
47  
48  
49  
50  
51  
52  
53  
54  
55  
56  
57  
58  
59  
60
7. Mortensen, P.M.; Grunwaldt, J. D.; Jensen, P. A.; Knudsen, K. G.; Jensen, A. D. A review of catalytic upgrading of bio-oil to engine fuels. *Appl. Catal. A-Gen.* **2011**, *407* (1-2), 1-19.
  8. Zacher, A.H.; Olarte, M. V.; Santosa, D. M.; Elliott, D. C.; Jones, S. B. A review and perspective of recent bio-oil hydrotreating research. *Green Chem.* **2014**, *16* (2), 491-515.
  9. Garcia-Perez, M.; Shen, J.; Wang, X. S.; Li, C. Z. Production and fuel properties of fast pyrolysis oil/bio-diesel blends. *Fuel Process. Technol.* **2010**, *91* (3), 296-305.
  10. Kim, T.Y., Lee, S.; Kang K., Performance and emission characteristics of a high-compression-ratio diesel engine fueled with wood pyrolysis oil-butanol blended fuels. *Energy* **2015**, *93* (2), 2241-2250.
  11. Zhang, M.; Wu, H. Phase Behavior and Fuel Properties of Bio-Oil/Glycerol/Methanol Blends. *Energy Fuels* **2016**, *30* (9), pp 6863–6880 **2014**, *28* (7), 4650-4656.
  12. Krutof, A.; Hawboldt, K. Blends of pyrolysis oil, petroleum, and other bio-based fuels: A review. *Renew. Sustainable Energy Rev.* **2016**, *59*, 406-419.
  13. Chong, K.J.; Bridgwater, A.V. Fast Pyrolysis Oil Fuel Blend for Marine Vessels. *Environ. Prog. Sustain. Energy*, 2016.
  14. Alcala, A.; Bridgwater, A.V. Upgrading fast pyrolysis liquids: Blends of biodiesel and pyrolysis oil. *Fuel* **2013**, *109* (0), 417-426.
  15. Staš, M.; Kubička, D.; Chudoba, J.; Pospíšil, M. Overview of Analytical Methods Used for Chemical Characterization of Pyrolysis Bio-oil. *Energy Fuels* **2014**, *28* (1), 385-402.
  16. Oasmaa, A.; van de Beld, B.; Saari, P.; Elliott, D. C.; Solantausta, Y. Norms, Standards, and Legislation for Fast Pyrolysis Bio-oils from Lignocellulosic Biomass. *Energy Fuels* **2015**, *29* (4), 2471-2484.

- 1  
2  
3 17. Garcia-Perez, M.; Chaala, A.; Pakdel, H.; Kretschmer, D.; Roy, C. Characterization of  
4 bio-oils in chemical families. *Biomass Bioenerg.* **2007**, *31* (4), 222-242.  
5  
6  
7  
8 18. Mullen, C.A. and A.A. Boateng, Chemical composition of bio-oils produced by fast  
9 pyrolysis of two energy crops. *Energy Fuels* **2008**, *22* (3), 2104-2109.  
10  
11  
12 19. Choi, Y. S.; Johnston, P. A.; Brown, R. C.; Shanks, B. H., Lee, K.-H. Detailed  
13 characterization of red oak-derived pyrolysis oil: Integrated use of GC, HPLC, IC, GPC and  
14 Karl-Fischer. *J. Anal. Appl. Pyrol.* **2014**, *110*, 147-154.  
15  
16  
17 20. Mullen, C.A.; Strahan G.D.; Boateng A.A. Characterization of Various Fast-Pyrolysis  
18 Bio-Oils by NMR Spectroscopy. *Energy Fuels* **2009**, *23* (5), 2707-2718.  
19  
20  
21 21. Hao, N.; Ben, H.; Yoo, C. G.; Adhikari, S.; Ragauskas, A. J. Review of NMR  
22 Characterization of Pyrolysis Oils. *Energy Fuels* **2016**, *30* (9), 6863-6880.  
23  
24  
25 22. Zhang, F. Brüsweiler, R. Spectral Deconvolution of Chemical Mixtures by Covariance  
26 NMR. *ChemPhysChem* **2004**, *5* (6), 794-796.  
27  
28  
29 23. Barker, P.; Freeman, R. Pulsed field gradients in NMR. An alternative to phase cycling.  
30 *J. Magn. Reson.* **1985**, *64* (2), 334-338.  
31  
32  
33 24. Johnson, C.S. Diffusion ordered nuclear magnetic resonance spectroscopy: principles and  
34 applications. *Prog. Nucl. Magn. Reson. Spectrosc.* **1999**, *34* (3-4), 203-256.  
35  
36  
37 25. Stejskal, E.O.; Tanner J.E. Spin diffusion measurements: spin echoes in the presence of a  
38 time-dependent field gradient. *J. Chem. Phys.* **1965**, *42* (1), 288-292.  
39  
40  
41 26. Lambert, J.; Hergenroder, R.; Suter, D.; Deckert, V. Probing liquid-liquid interfaces with  
42 spatially resolved NMR spectroscopy. *Angew. Chem. Int. Ed.* **2009**, *48* (34), 6343-63435.  
43  
44  
45  
46  
47  
48  
49  
50  
51  
52  
53  
54  
55  
56  
57  
58  
59  
60

- 1  
2  
3 27. Mantel, C.; Bayle, P-A.; Hediger, S.; Berthon, C.; Bardet, M. Study of liquid–liquid  
4 interfaces by an easily implemented localized NMR sequence. *Magn. Reson. Chem.* **2010**, *48* (8),  
5 600-606.  
6  
7  
8  
9  
10 28. Allen, J.; Damodaran, K. High-resolution slice selection NMR for the measurement of  
11 CO<sub>2</sub> diffusion under non-equilibrium conditions. *Magn. Reson. Chem.* **2015**, *53* (3), 200-202.  
12  
13 29. Garcia-Aparicio, C.; Quijada-Garrido, I.; Garrido, L. Diffusion of small molecules in a  
14 chitosan/water gel determined by proton localized NMR spectroscopy. *J. Colloid Interface Sci.*  
15 **2012**, *368* (1), 14-20.  
16  
17  
18  
19  
20 30. Mitrev, Y.; Simova, S.; Jeannerat, D. NMR analysis of weak molecular interactions using  
21 slice-selective experiments via study of concentration gradients in agar gels. *Chem. Commun.*  
22 **2016**, *52*, 5418-5420.  
23  
24  
25  
26  
27 31. Poppler, A. C.; Frischkorn, S.; Stalke, D.; John, M. Toluene and lithium amide diffusion  
28 into polystyrene: a slice-selective NMR-spectroscopic study. *ChemPhysChem* **2013**, *14* (13),  
29 3103-3107.  
30  
31  
32  
33  
34 32. Niklas, T., Stalke D.; John, M. Single-shot titrations and reaction monitoring by slice-  
35 selective NMR spectroscopy. *Chem. Commun.* **2015**, *51* (7), 1275-1277.  
36  
37  
38  
39  
40 33. Krachkovskiy, S. A.; Pauric, A. D.; Halalay, I. C.; Goward, G. R. Slice-Selective NMR  
41 Diffusion Measurements: A Robust and Reliable Tool for In Situ Characterization of Ion-  
42 Transport Properties in Lithium-Ion Battery Electrolytes. *J. Phys. Chem. Lett.* **2013**, *4* (22),  
43 3940-3944.  
44  
45  
46  
47  
48  
49 34. Emsley, L.; Bodenhausen, G. Gaussian pulse cascades: New analytical functions for  
50 rectangular selective inversion and in-phase excitation in NMR. *Chem. Phys. Lett.* **1990**, *165* (6),  
51 469-476.  
52  
53  
54  
55  
56  
57  
58  
59  
60

- 1  
2  
3 35. Fulmer, G. R.; Miller, A. J. M.; Sherden, N. H.; Gottlieb, H. E.; Nudelman, A.; Stoltz, B.  
4  
5 M.; Bercaw, J. E.; Goldberg, K. I. NMR Chemical Shifts of Trace Impurities: Common  
6  
7 Laboratory Solvents, Organics, and Gases in Deuterated Solvents Relevant to the Organometallic  
8  
9 Chemist. *Organometallics*, **2010**, *29* (9), 2176-2179.
- 10  
11  
12 36. Phan, C. M.; Allen, B.; Peters, L. B.; Le, T. N.; Tade, M. O. Can Water Float on Oil?  
13  
14 *Langmuir*, **2012**, *28* (10), 4609-4613.
- 15  
16  
17 37. Huang, F.; Pan, S.; Pu, Y.; Ben, H.; Ragauskas, A. J. <sup>19</sup>F NMR spectroscopy for the  
18  
19 quantitative analysis of carbonyl groups in biooils. *RSC Adv.* **2014**, *4* (34), 17743-17747.
- 20  
21  
22 38. David, K.; Kosa, M.; Williams, A.; Mayor, R.; Realff, M.; Muzzy, J.; Ragauskas, A. <sup>31</sup>P-  
23  
24 NMR analysis of bio-oils obtained from the pyrolysis of biomass. *Biofuels* **2010**, *1* (6), 839-845.
- 25  
26  
27 39. Halliday, N.A.; Peet, A.C.; Britton, M.M.; Detection of pH in Microemulsions, without a  
28  
29 Probe Molecule, Using Magnetic Resonance. *J. Phys. Chem. B*, **2010**, *114* (43), 13745-13751.
- 30  
31  
32 40. Evans, R.; Deng, Z.; Rogerson, A. K.; McLachlan, A. S.; Richards, J. J.; Nilsson, M.;  
33  
34 Morris, G. A. Quantitative interpretation of diffusion-ordered NMR spectra: can we rationalize  
35  
36 small molecule diffusion coefficients? *Angew. Chem. Int. Ed.* **2013**, *52* (11), 3199-3202.
- 37  
38  
39 41. Li, W.; Kagan, G.; Hopson, R.; Williard, P. G. Measurement of Solution Viscosity via  
40  
41 Diffusion-Ordered NMR Spectroscopy (DOSY). *J. Chem. Edu.* **2011**, *88* (9), 1331-1335.
- 42  
43  
44 42. Aguilar, J. A.; Nilsson, M.; Bodenhausen, G.; Morris, G. A. Spin echo NMR spectra  
45  
46 without J modulation. *Chem. Commun.* **2012**, *48* (6), 811-3.
- 47  
48  
49 43. Esturau, N.; J.F. Espinosa, Optimization of Diffusion-Filtered NMR Experiments for  
50  
51 Selective Suppression of Residual Nondeuterated Solvent and Water Signals from <sup>1</sup>H NMR  
52  
53 Spectra of Organic Compounds. *J. Org. Chem.* **2006**, *71* (11), 4103-4110.
- 54  
55  
56  
57  
58  
59  
60

## GRAPHICAL ABSTRACT





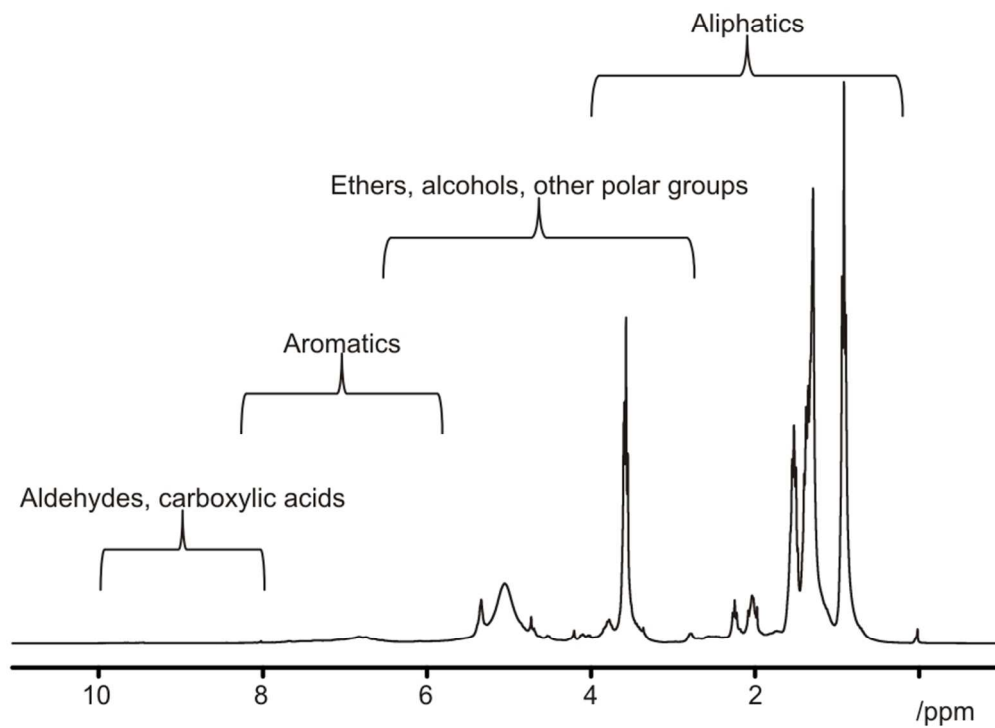


Figure1.  $^1\text{H}$  NMR spectra of a blended fuel sample, with characteristic chemical shift regions of functional groups indicated.



Figure 2. Photograph of two typical blended fuel samples.

67x71mm (220 x 220 DPI)

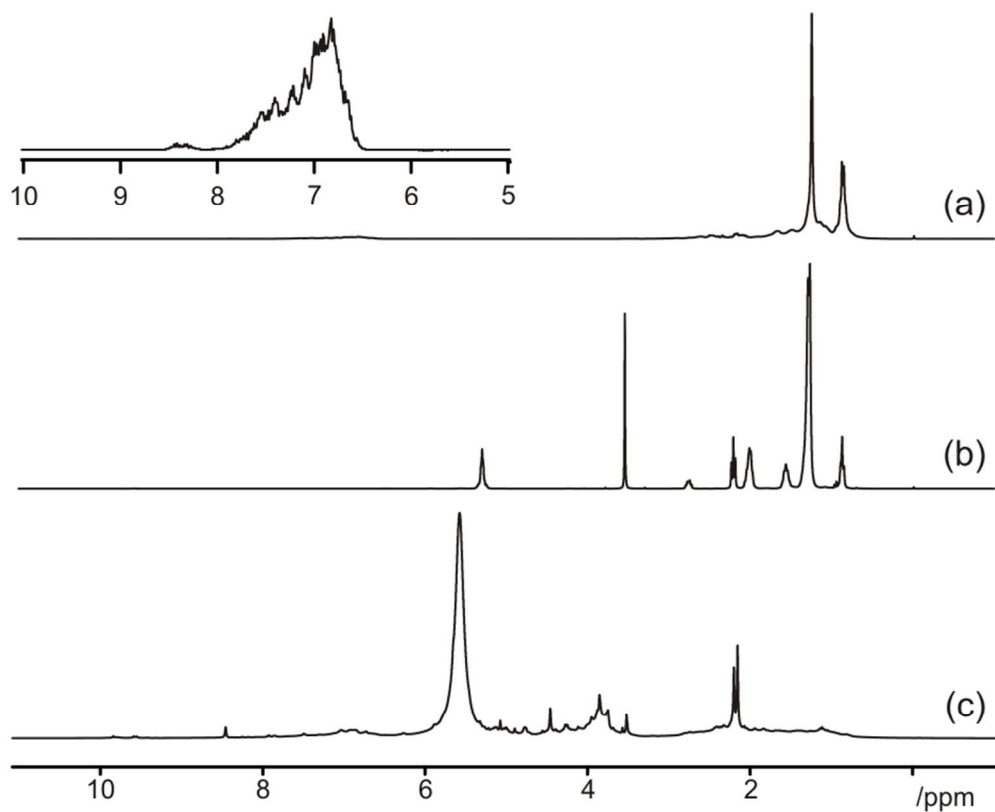


Figure 3.  $1\text{D } ^1\text{H}$  NMR spectra of raw components (a) marine gas oil (b) FAME and (c) bio-oil used in blended bio-fuel mixtures. Inset in Fig. 3 (a) shows a hundred fold expansion of the region between 5 and 10 ppm, indicating the signals due to aromatic species in the marine gas oil.

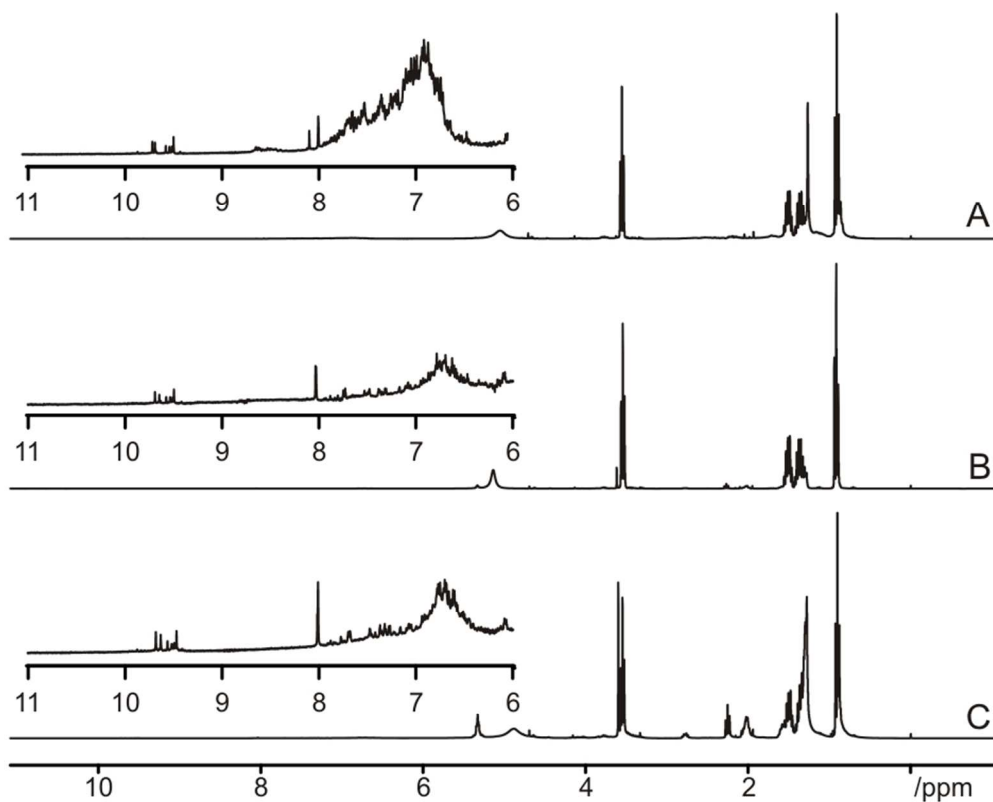


Figure 4. 1D  $^1\text{H}$  NMR spectra of three-component unseparated samples, A, B and C.

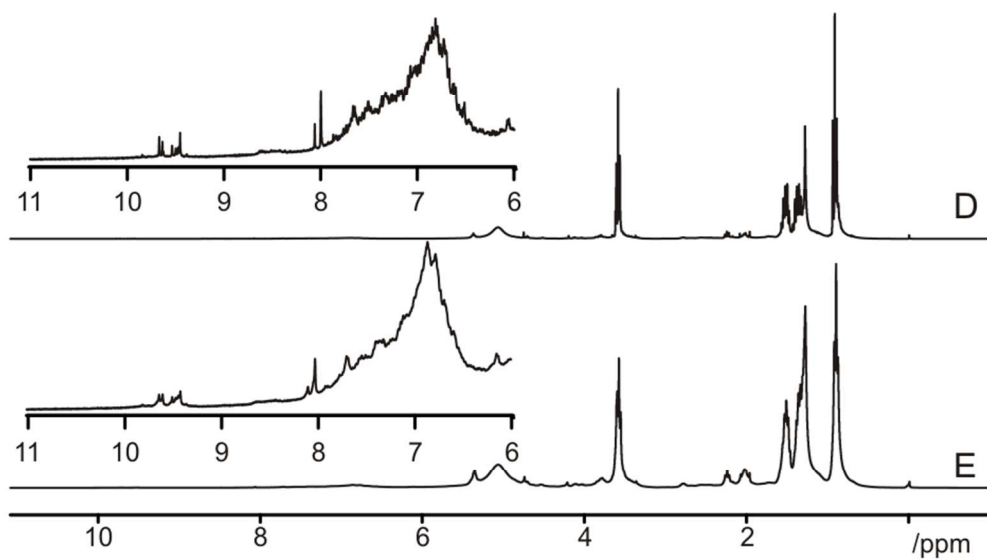
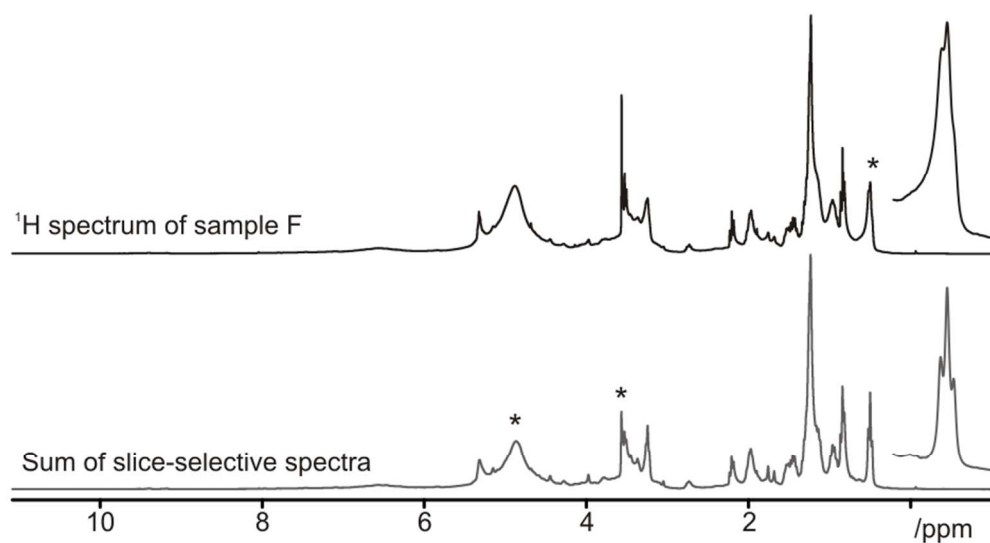


Figure 5. 1D  $^1\text{H}$  NMR spectra of four-component unseparated samples, D and E.



26  
27  
28  
29  
30  
31  
32  
33  
34  
35  
36  
37  
38  
39  
40  
41  
42  
43  
44  
45  
46  
47  
48  
49  
50  
51  
52  
53  
54  
55  
56  
57  
58  
59  
60

Figure 6. Comparison of the sum of slice-selective <sup>1</sup>H NMR spectra of upper and lower levels of Sample F with <sup>1</sup>H NMR spectrum of complete sample. Butanol peak at 0.55 ppm enlarged to highlight differences in resolution between the two techniques.

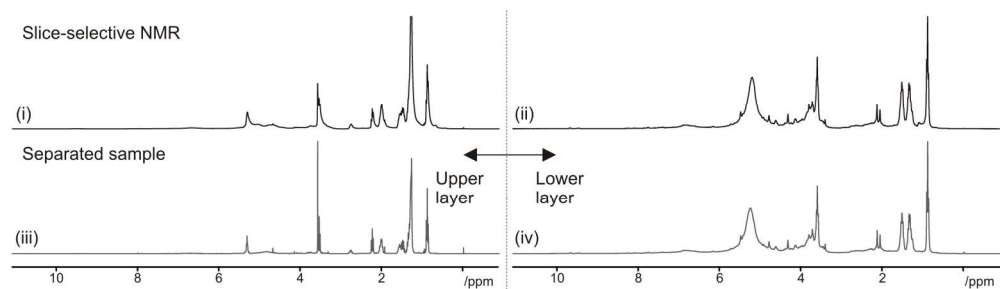
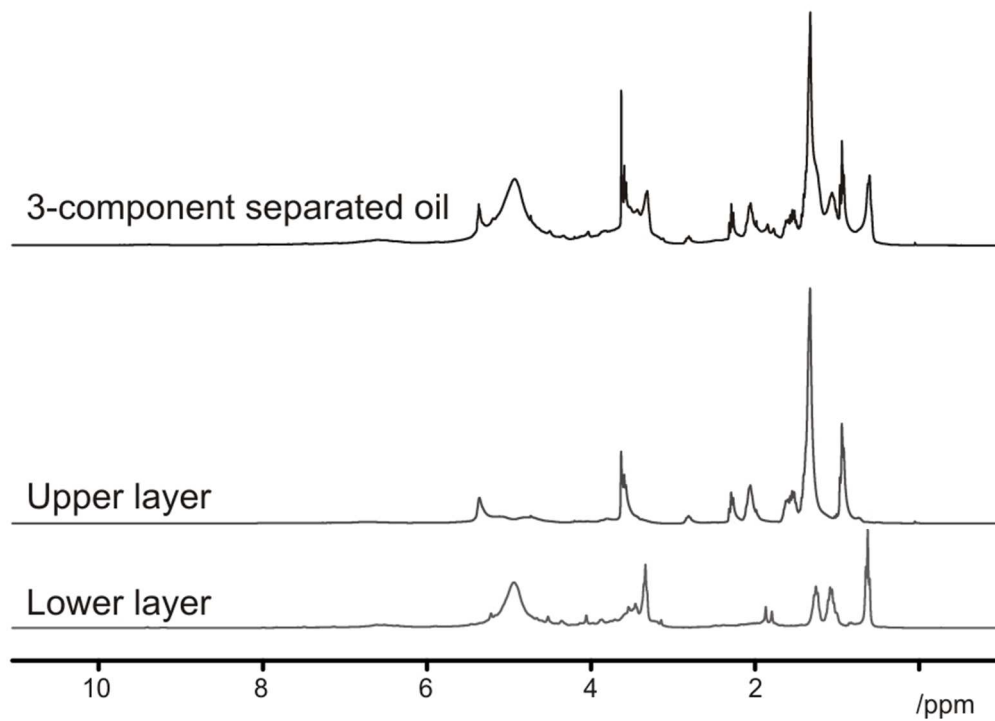


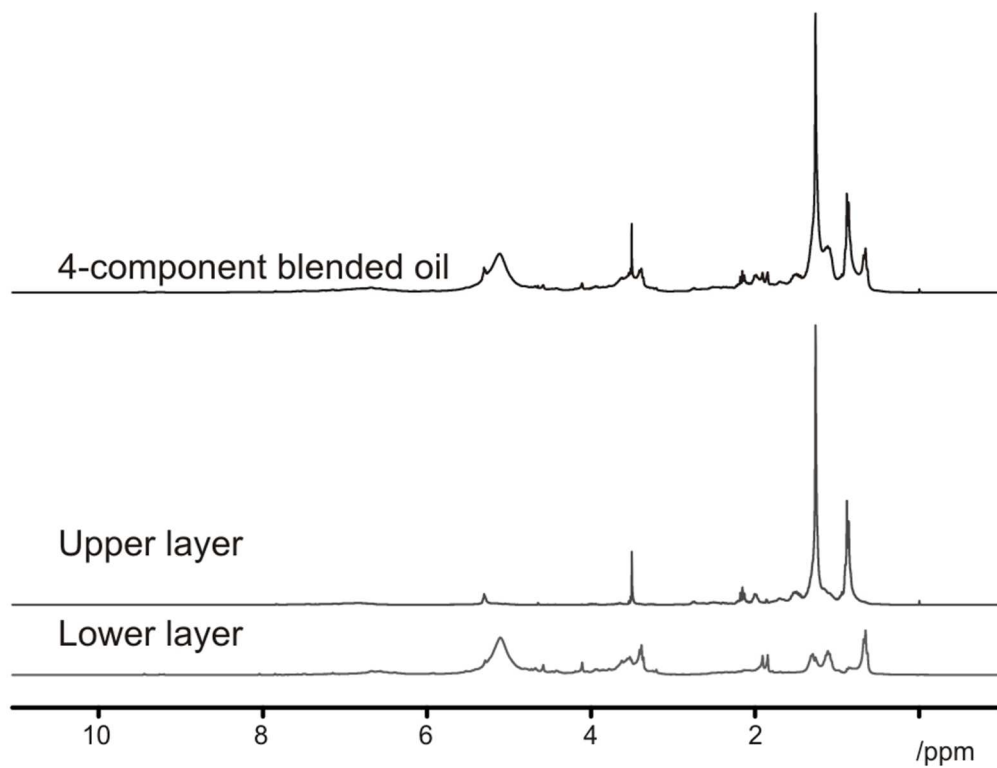
Figure 7. Comparison of slice-selective  $^1\text{H}$  NMR spectra of (i) upper and (ii) lower levels of Sample F with  $^1\text{H}$  NMR spectra of the (iii) upper and (iv) lower levels of a physically separated sample.



34 Figure 8. Slice-selective  $^1\text{H}$  NMR spectra of Sample F, a phase-separated 3-component oil sample.

35  
36  
37  
38  
39  
40  
41  
42  
43  
44  
45  
46  
47  
48  
49  
50  
51  
52  
53  
54  
55  
56  
57  
58  
59  
60





34 Figure 9. slice-selective  $^1\text{H}$  NMR of Sample G, a phase-separated 4-component oil sample.

35  
36  
37  
38  
39  
40  
41  
42  
43  
44  
45  
46  
47  
48  
49  
50  
51  
52  
53  
54  
55  
56  
57  
58  
59  
60

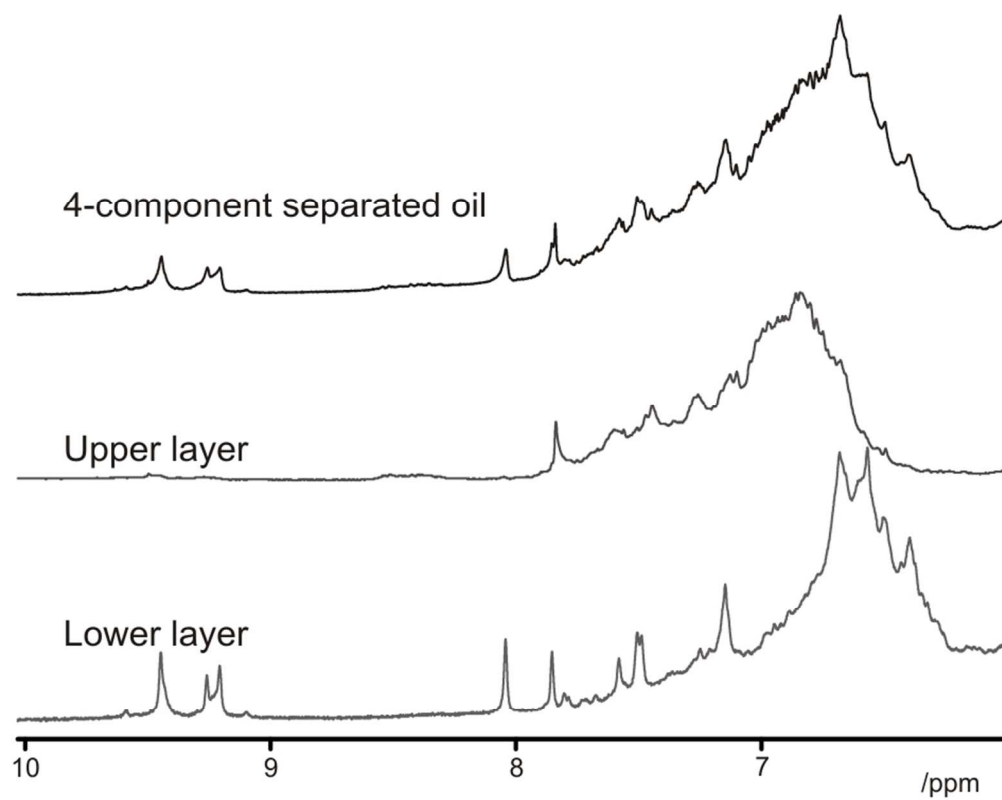
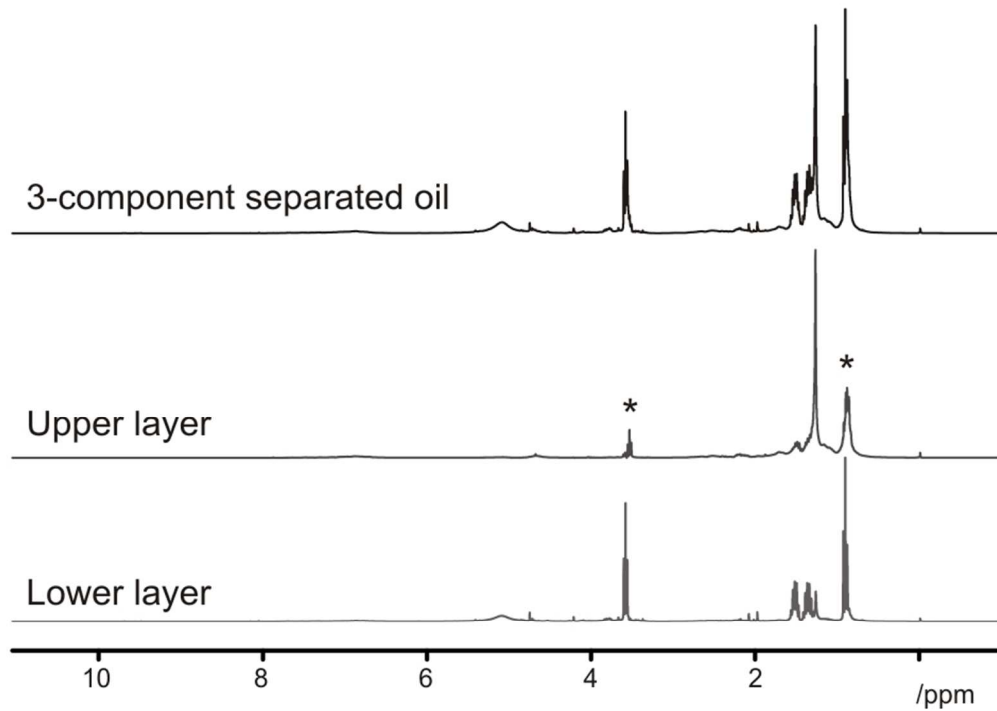


Figure 10. Slice-selective  $^1\text{H}$  NMR of aromatic region of Sample G, a phase-separated 4-component oil sample.



34 Figure 11. Slice-selective  $^1\text{H}$  NMR of Sample H, a phase-separated 3-component oil sample.

35  
36  
37  
38  
39  
40  
41  
42  
43  
44  
45  
46  
47  
48  
49  
50  
51  
52  
53  
54  
55  
56  
57  
58  
59  
60